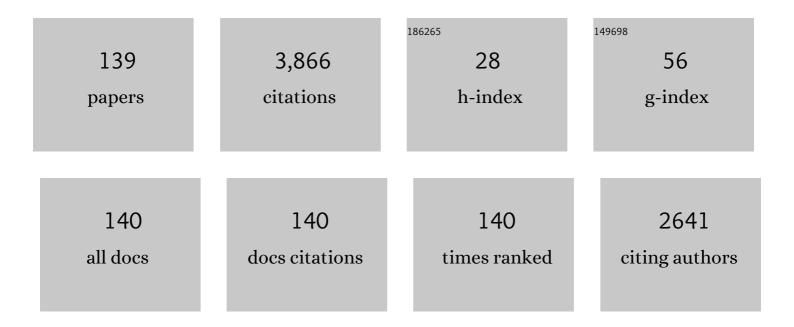
List of Publications by Year in descending order

Source: https://exaly.com/author-pdf/1485840/publications.pdf Version: 2024-02-01



#	Article	lF	CITATIONS
1	Heterogeneous precipitation behavior and stacking-fault-mediated deformation in a CoCrNi-based medium-entropy alloy. Acta Materialia, 2017, 138, 72-82.	7.9	553
2	Outstanding tensile properties of a precipitation-strengthened FeCoNiCrTi0.2 high-entropy alloy at room and cryogenic temperatures. Acta Materialia, 2019, 165, 228-240.	7.9	373
3	Pure-Shuffle Nucleation of Deformation Twins in Hexagonal-Close-Packed Metals. Materials Research Letters, 2013, 1, 126-132.	8.7	181
4	Strengthening of nanoprecipitations in an annealed Al0.5CoCrFeNi high entropy alloy. Materials Science & Engineering A: Structural Materials: Properties, Microstructure and Processing, 2016, 671, 82-86.	5.6	158
5	Obligatory and facilitative allelic variation in the DNA methylome within common disease-associated loci. Nature Communications, 2018, 9, 8.	12.8	107
6	Characterization of BCC phases in AlCoCrFeNiTix high entropy alloys. Materials Letters, 2015, 138, 78-80.	2.6	103
7	Enhanced mechanical properties of a CoCrFeNi high entropy alloy by supercooling method. Materials and Design, 2016, 95, 183-187.	7.0	99
8	Integrating data mining and machine learning to discover high-strength ductile titanium alloys. Acta Materialia, 2021, 202, 211-221.	7.9	85
9	Microstructure and properties of bulk Al0.5CoCrFeNi high-entropy alloy by cold rolling and subsequent annealing. Materials Science & Engineering A: Structural Materials: Properties, Microstructure and Processing, 2018, 729, 141-148.	5.6	74
10	Effect of a weak transverse magnetic field on solidification structure during directional solidification. Acta Materialia, 2014, 64, 367-381.	7.9	67
11	Anomalous structural dynamics in liquid Al80Cu20: An ab initio molecular dynamics study. Acta Materialia, 2015, 97, 75-85.	7.9	62
12	The characteristics of serration in Al0.5CoCrFeNi high entropy alloy. Materials Science & Engineering A: Structural Materials: Properties, Microstructure and Processing, 2017, 702, 96-103.	5.6	62
13	Tribological Behavior of AlCoCrFeNi(Ti0.5) High Entropy Alloys under Oil and MACs Lubrication. Journal of Materials Science and Technology, 2016, 32, 470-476.	10.7	61
14	Size-dependent role of S phase in pitting initiation of 2024Al alloy. Corrosion Science, 2016, 105, 183-189.	6.6	60
15	Multiple twins of a decagonal approximant embedded in S-Al2CuMg phase resulting in pitting initiation of a 2024Al alloy. Acta Materialia, 2015, 82, 22-31.	7.9	59
16	The FCC to BCC phase transformation kinetics in an Al0.5CoCrFeNi high entropy alloy. Journal of Alloys and Compounds, 2017, 710, 144-150.	5.5	59
17	Microstructure and mechanical properties of non-equilibrium solidified CoCrFeNi high entropy alloy. Materials Chemistry and Physics, 2018, 210, 192-196.	4.0	57
18	Seaweed eutectic-dendritic solidification pattern in a CoCrFeNiMnPd eutectic high-entropy alloy. Intermetallics, 2017, 85, 74-79.	3.9	55

#	Article	IF	CITATIONS
19	Nanophase precipitation and strengthening in a dual-phase Al0.5CoCrFeNi high-entropy alloy. Journal of Materials Science and Technology, 2021, 72, 1-7.	10.7	51
20	Microstructure and Tribological Properties of AlCoCrFeNiTi0.5 High-Entropy Alloy in Hydrogen Peroxide Solution. Metallurgical and Materials Transactions A: Physical Metallurgy and Materials Science, 2014, 45, 201-207.	2.2	49
21	Microstructure characterization of CoCrFeNiMnPd eutectic high-entropy alloys. Journal of Alloys and Compounds, 2018, 731, 600-611.	5.5	49
22	Local lattice distortion mediated formation of stacking faults in Mg alloys. Acta Materialia, 2019, 170, 231-239.	7.9	45
23	Tribological behavior of AlCoCrCuFeNi and AlCoCrFeNiTi0.5 high entropy alloys under hydrogen peroxide solution against different counterparts. Tribology International, 2015, 92, 203-210.	5.9	39
24	Crystallization kinetics of Cu38Zr46Ag8Al8 bulk metallic glass in different heating conditions. Journal of Non-Crystalline Solids, 2014, 404, 7-12.	3.1	35
25	Effect of strong magnetic field on the microstructure and mechanical-magnetic properties of AlCoCrFeNi high-entropy alloy. Journal of Alloys and Compounds, 2020, 820, 153407.	5.5	34
26	Tailoring mechanical and magnetic properties of AlCoCrFeNi high-entropy alloy via phase transformation. Journal of Materials Science and Technology, 2021, 73, 83-90.	10.7	34
27	Corrosive and tribological behaviors of AlCoCrFeNi-M high entropy alloys under 90†wt. % H2O2 solution. Tribology International, 2019, 131, 24-32.	5.9	32
28	Liquid-phase separation in undercooled CoCrCuFeNi high entropy alloy. Intermetallics, 2017, 86, 110-115.	3.9	30
29	Strain-rate-dependent deformation behavior in a Ti-based bulk metallic glass composite upon dynamic deformation. Journal of Alloys and Compounds, 2015, 639, 131-138.	5.5	28
30	Liquid–liquid structure transition and nucleation in undercooled Co-B eutectic alloys. Applied Physics A: Materials Science and Processing, 2017, 123, 1.	2.3	27
31	Microstructure and Mechanical Properties of CoCrFeMnNiSnx High-Entropy Alloys. Metals and Materials International, 2020, 26, 292-301.	3.4	27
32	Optimizing mechanical and magnetic properties of AlCoCrFeNi high-entropy alloy via FCC to BCC phase transformation. Journal of Materials Science and Technology, 2021, 86, 117-126.	10.7	27
33	Deformation behavior of a Ti-based bulk metallic glass composite with excellent cryogenic mechanical properties. Materials & Design, 2014, 53, 737-740.	5.1	26
34	Hot Deformation Behavior of As-Cast and Homogenized Al0.5CoCrFeNi High Entropy Alloys. Metals, 2016, 6, 277.	2.3	26
35	Evolution of microstructure and hardness in a dual-phase Al0.5CoCrFeNi high-entropy alloy with different grain sizes. Rare Metals, 2020, 39, 156-161.	7.1	25
36	Enhancing mechanical properties of Al0.25CoCrFeNi high-entropy alloy via cold rolling and subsequent annealing. Journal of Alloys and Compounds, 2020, 830, 154645.	5.5	25

#	Article	IF	CITATIONS
37	Fully Recrystallized Al0.5CoCrFeNi High-Entropy Alloy Strengthened by Nanoscale Precipitates. Metals and Materials International, 2019, 25, 1145-1150.	3.4	24
38	Influence of high magnetic field on the liquid-liquid phase separation behavior of an undercooled Cu–Co immiscible alloy. Journal of Alloys and Compounds, 2020, 842, 155502.	5.5	24
39	Temperature dependent deformation mechanisms of Al0.3CoCrFeNi high-entropy alloy, starting from serrated flow behavior. Journal of Alloys and Compounds, 2018, 757, 39-43.	5.5	22
40	Nucleation of supercooled Co melts under a high magnetic field. Materials Chemistry and Physics, 2019, 225, 133-136.	4.0	22
41	On discussion of the applicability of local Avrami exponent: Errors and solutions. Materials Letters, 2009, 63, 1153-1155.	2.6	20
42	Determination of kinetic parameters during isochronal crystallization of Ti40Zr25Ni8Cu9Be18 metallic glass. Journal of Alloys and Compounds, 2009, 479, 835-839.	5.5	20
43	Experimental platform for solidification and <i>in-situ</i> magnetization measurement of undercooled melt under strong magnetic field. Review of Scientific Instruments, 2015, 86, 025102.	1.3	19
44	Strain rate response of a Ti-based metallic glass composite at cryogenic temperature. Materials Letters, 2014, 117, 228-230.	2.6	18
45	Rheological behavior of Cu–Zr-based metallic glass in the supercooled liquid region. Journal of Alloys and Compounds, 2014, 592, 189-195.	5.5	18
46	Magnetic field enhanced phase precipitation in an undercooled Co–Sn alloy. Materials Letters, 2015, 139, 288-291.	2.6	18
47	Tensile deformation mechanisms of an in-situ Ti-based metallic glass matrix composite at cryogenic temperature. Scientific Reports, 2016, 6, 32287.	3.3	18
48	Strong magnetic field effect on the nucleation of a highly undercooled Co-Sn melt. Scientific Reports, 2017, 7, 4958.	3.3	18
49	Coupling effects of high magnetic field and annealing on the microstructure evolution and mechanical properties of additive manufactured Ti–6Al–4V. Materials Science & Engineering A: Structural Materials: Properties, Microstructure and Processing, 2021, 824, 141815.	5.6	18
50	Dendrite size dependence of mechanical properties of in-situ Ti-based bulk metallic glass matrix composites. Materials Science & Engineering A: Structural Materials: Properties, Microstructure and Processing, 2017, 704, 77-81.	5.6	17
51	Insight into solid-solution strengthened bulk and stacking faults properties in Ti alloys: a comprehensive first-principles study. Journal of Materials Science, 2018, 53, 7493-7505.	3.7	17
52	Hot Deformation and Subsequent Annealing on the Microstructure and Hardness of an Al0.3CoCrFeNi High-entropy Alloy. Acta Metallurgica Sinica (English Letters), 2021, 34, 1527-1536.	2.9	17
53	An integral fitting method for analyzing the isochronal transformation kinetics: Application to the crystallization of a Ti-based amorphous alloy. Journal of Physics and Chemistry of Solids, 2009, 70, 1448-1453.	4.0	16
54	Anomalous magnetism and normal field instability in supercooled liquid cobalt. Applied Physics Letters, 2014, 105, 144101.	3.3	16

#	Article	IF	CITATIONS
55	Formation of a hexagonal closed-packed phase in Al0.5CoCrFeNi high entropy alloy. MRS Communications, 2017, 7, 879-884.	1.8	16
56	When a defect is a pathway to improve stability: a case study of the L12 Co3TM superlattice intrinsic stacking fault. Journal of Materials Science, 2019, 54, 13609-13618.	3.7	16
57	Phase Separation and Microstructure Evolution of Zr48Cu36Ag8Al8 Bulk Metallic Glass in the Supercooled Liquid Region. Rare Metal Materials and Engineering, 2016, 45, 567-570.	0.8	15
58	Numerical Simulation and Process Optimization of Vacuum Investment Casting for Be–Al Alloys. International Journal of Metalcasting, 2019, 13, 74-81.	1.9	15
59	Liquidâ °'liquid structure transition in metallic melt and its impact on solidification: A review. Transactions of Nonferrous Metals Society of China, 2020, 30, 2293-2310.	4.2	15
60	Revealing foundations of the intergranular corrosion of 5XXX and 6XXX Al alloys. Materials Letters, 2020, 271, 127767.	2.6	15
61	Electronic structures and properties of TiAl/Ti2AlNb heterogeneous interfaces: A comprehensive first-principles study. Intermetallics, 2021, 133, 107173.	3.9	15
62	Tensile properties and deformation micromechanism of Ti-based metallic glass composite containing impurity elements. Journal of Alloys and Compounds, 2019, 784, 220-230.	5.5	14
63	High-throughput investigations of configurational-transformation-dominated serrations in CuZr/Cu nanolaminates. Journal of Materials Science and Technology, 2020, 53, 192-199.	10.7	14
64	Tailoring the microstructure, magnetic properties and interaction mechanisms of Alnico-Ta alloys by magnetic field treatment. Journal of Alloys and Compounds, 2021, 857, 157586.	5.5	14
65	Kinetic analysis of the isochronal crystallization of Ti40Zr25Ni8Cu9Be18 metallic glass. Journal of Non-Crystalline Solids, 2009, 355, 420-424.	3.1	13
66	Deformation behavior of a Ti-based bulk metallic glass composite in the supercooled liquid region. Materials and Design, 2016, 90, 595-600.	7.0	13
67	Effect of liquid–liquid structure transition on the nucleation in undercooled Co–Sn eutectic alloy. Materials Chemistry and Physics, 2016, 170, 261-265.	4.0	13
68	Tune the mechanical properties of Ti-based metallic glass composites by additions of nitrogen. Materials Science & Engineering A: Structural Materials: Properties, Microstructure and Processing, 2017, 694, 93-97.	5.6	13
69	Effect of Cold Rolling on the Phase Transformation Kinetics of an Al0.5CoCrFeNi High-Entropy Alloy. Entropy, 2018, 20, 917.	2.2	13
70	Influence of oxygen on microstructure and phase transformation in high Nb containing TiAl alloys. Materials Letters, 2012, 83, 198-201.	2.6	12
71	Overheating dependent undercooling in a hypoeutectic Co–B alloy. Materials Chemistry and Physics, 2015, 149-150, 17-20.	4.0	12
72	Quasi-static and dynamic deformation of an in-situ Ti-based metallic glass composite in supercooled liquid region. Journal of Alloys and Compounds, 2016, 679, 239-246.	5.5	12

#	Article	IF	CITATIONS
73	Magnetic-field-induced chain-like assemblies of the primary phase during non-equilibrium solidification of a Co-B eutectic alloy: Experiments and modeling. Journal of Alloys and Compounds, 2020, 815, 152446.	5.5	12
74	Reexaminations of the effects of magnetic field on the nucleation of undercooled Cu melt. Japanese Journal of Applied Physics, 2016, 55, 105601.	1.5	11
75	Diffusion Bonding between Zr-Based Metallic Glass and Copper. Rare Metal Materials and Engineering, 2016, 45, 42-45.	0.8	11
76	Liquid-liquid phase separation in immiscible Cu-Co alloy. Materials Letters, 2020, 268, 127585.	2.6	11
77	Microstructure evolution of peritectic Al–18 at.% Ni alloy directionally solidified in high magnetic fields. Journal of Materials Science and Technology, 2021, 76, 51-59.	10.7	11
78	Effect of high magnetic field assisted heat treatment on microstructure and properties of AlCoCrCuFeNi high-entropy alloy. Materials Letters, 2021, 303, 130540.	2.6	11
79	Microstructure, phase and microhardness distribution of laser-deposited Ni-based amorphous coating. International Journal of Surface Science and Engineering, 2010, 4, 296.	0.4	10
80	Evidence for the structure transition in a liquid Co–Sn alloy by in-situ magnetization measurement. Materials Letters, 2015, 145, 261-263.	2.6	10
81	Enhanced mechanical properties of Ti-based metallic glass composites prepared under medium vacuum system. Journal of Non-Crystalline Solids, 2015, 413, 15-19.	3.1	10
82	The Effect of Thermal Cycling Treatments on the Thermal Stability and Mechanical Properties of a Ti-Based Bulk Metallic Glass Composite. Metals, 2016, 6, 274.	2.3	10
83	Temperature-induced structure transition in a liquid Co-B eutectic alloy. Materials Letters, 2019, 234, 351-353.	2.6	10
84	Microstructure and properties of AlCoCrCuFeNi high-entropy alloy solidified under high magnetic field. Materials Letters, 2021, 285, 129182.	2.6	10
85	Crystallization and compressive behaviors of Ti40Zr25Ni8Cu9Be18 BMG cast from different liquid states. Intermetallics, 2012, 28, 45-50.	3.9	9
86	Microstructure Evolution of a Ti-Based Bulk Metallic Glass Composite During Deformation. Journal of Materials Engineering and Performance, 2015, 24, 748-753.	2.5	9
87	Instability Pattern Formation in a Liquid Metal under High Magnetic Fields. Scientific Reports, 2017, 7, 2248.	3.3	9
88	Transition from hypereutectic to hypoeutectic for rapid solidification in an undercooled Co-B alloy. Journal of Crystal Growth, 2018, 499, 98-105.	1.5	9
89	Effect of Solidification on Microstructure and Properties of FeCoNi(AlSi)0.2 High-Entropy Alloy Under Strong Static Magnetic Field. Entropy, 2018, 20, 275.	2.2	9
90	The effect of high magnetic field on the microstructure evolution of a Cu-Co alloy during non-equilibrium solidification. Journal of Crystal Growth, 2019, 515, 78-82.	1.5	9

#	Article	IF	CITATIONS
91	Deformation behaviors of a Ti-based bulk metallic glass composite in the dendrite softening region. Materials Science & Engineering A: Structural Materials: Properties, Microstructure and Processing, 2016, 653, 1-7.	5.6	8
92	A novel strategy for enhancing mechanical performance of Al0.5CoCrFeNi high-entropy alloy via high magnetic field. Materials Letters, 2019, 240, 250-252.	2.6	8
93	Composition dependent characteristic transition temperatures of Co-B melts. Journal of Non-Crystalline Solids, 2019, 522, 119583.	3.1	8
94	Interstitial triggered grain boundary embrittlement of Al–X (X = H, N and O). Computational Materials Science, 2019, 163, 241-247.	3.0	8
95	Thermal–Mechanical Processing and Strengthen in AlxCoCrFeNi High-Entropy Alloys. Frontiers in Materials, 2021, 7, .	2.4	8
96	Local orders, lattice distortions, and electronic structure dominated mechanical properties of (ZrHfTaM1M2)C (M = Nb, Ti, V). Journal of the American Ceramic Society, 2022, 105, 4260-4276.	3.8	8
97	Tailoring the magnetic properties and microstructure of Alnico 8 magnets by various Ti contents and processing conditions. Intermetallics, 2022, 143, 107486.	3.9	8
98	Interface characteristics of a Zr-based BMG/copper laminated composite. Surface and Interface Analysis, 2014, 46, 61-64.	1.8	7
99	Microstructure Evolution and Mechanical Properties of a Ti-Based Bulk Metallic Glass Composite. Journal of Materials Engineering and Performance, 2015, 24, 2354-2358.	2.5	7
100	Temperature dependent dynamic flow behavior of an in-situ Ti-based bulk metallic glass composite. Materials Science & Engineering A: Structural Materials: Properties, Microstructure and Processing, 2015, 627, 21-26.	5.6	7
101	Numerical modeling and experiment of counter-gravity casting for titanium alloys. International Journal of Advanced Manufacturing Technology, 2016, 85, 1877-1885.	3.0	7
102	Dry-sliding tribological properties of AlCoCrFeNiTi0.5 high-entropy alloy. Rare Metals, 2022, 41, 4266-4272.	7.1	7
103	Pitting Corrosion of Natural Aged Al–Mg–Si Extrusion Profile. Materials, 2019, 12, 1081.	2.9	7
104	Correlations between Shear Bands and Plasticity in Ti-Based Bulk Metallic Glass. Rare Metal Materials and Engineering, 2011, 40, 399-402.	0.8	6
105	A new microscopic coordinated deformation model of Ti-based bulk metallic composites during tensile deformation. Scripta Materialia, 2019, 172, 23-27.	5.2	6
106	Solidification of Immiscible Alloys under High Magnetic Field: A Review. Metals, 2021, 11, 525.	2.3	6
107	Effects of an ultra-high magnetic field up to 25 T on the phase transformations of undercooled Co-B eutectic alloy. Journal of Materials Science and Technology, 2021, 93, 79-88.	10.7	6
108	Lattice distortion-enhanced superlubricity of (Mo, X)S ₂ (X = Al, Ti, Cr and V) with moiré superlattice. Nanoscale, 2021, 13, 16234-16243.	5.6	6

#	Article	IF	CITATIONS
109	Formation of Stress-Induced Nano Defects in Shear Bands of Metallic Glasses. Rare Metal Materials and Engineering, 2010, 39, 941-944.	0.8	5
110	Thermal Stability and the Matrix Induced Brittleness in a Ti-based Bulk Metallic Glass Composite. Materials Research, 2015, 18, 83-88.	1.3	5
111	Correlation between diffusion and crystallization behaviors in Ni/Zr48Cu36Ag8Al8 diffusion couple. Journal of Non-Crystalline Solids, 2015, 417-418, 34-38.	3.1	5
112	Effect of strong static magnetic field on the microstructure and transformation temperature of Co–Ni–Al ferromagnetic shape memory alloy. Journal of Materials Science: Materials in Electronics, 2018, 29, 19491-19498.	2.2	5
113	Limitation of the Johnson-Mehl-Avrami equation for the kinetic analysis of crystallization in a Ti-based amorphous alloy. International Journal of Minerals, Metallurgy and Materials, 2010, 17, 307-311.	4.9	4
114	Microstructure Changes in Zr-Based Metallic Glass Induced by Ion Milling. Rare Metal Materials and Engineering, 2010, 39, 1693-1696.	0.8	4
115	Structure transitions near liquidus and the nucleation of undercooled melt of Ni–Cr–W superalloy. Physica B: Condensed Matter, 2014, 454, 8-14.	2.7	4
116	Study on Structural Transformation Behavior of a Ti-Based Bulk Metallic Glass by Thermal Expansion Method. Rare Metal Materials and Engineering, 2014, 43, 1047-1050.	0.8	4
117	Phase Transformation Kinetics of a FCC Al0.25CoCrFeNi High-Entropy Alloy during Isochronal Heating. Metals, 2018, 8, 1015.	2.3	4
118	Effect of Mn Addition on the Microstructures and Mechanical Properties of CoCrFeNiPd High Entropy Alloy. Entropy, 2019, 21, 288.	2.2	4
119	Effect of long-term aging treatment on the tensile strength and ductility of GH 605 superalloy. Progress in Natural Science: Materials International, 2022, 32, 375-384.	4.4	4
120	Diffusion behavior of Ni in Zr48Cu36Ag8Al8 bulk metallic glass within supercooled liquid region. Transactions of Nonferrous Metals Society of China, 2015, 25, 1171-1175.	4.2	3
121	Dynamic mechanical properties of a Ti-based metallic glass matrix composite. Journal of Applied Physics, 2015, 117, 155102.	2.5	3
122	Tribological Behavior of 1Cr18Ni9Ti Steel under Hydrogen Peroxide Solution against Different Ceramic Counterparts. Rare Metal Materials and Engineering, 2016, 45, 593-598.	0.8	3
123	The cryogenic mechanical property deviation of Ti-based bulk metallic glass composite induced by interstitial element. Journal of Non-Crystalline Solids, 2020, 542, 120105.	3.1	3
124	Effect of High Strain Rate on Adiabatic Shearing of α+β Dual-Phase Ti Alloy. Materials, 2021, 14, 2044.	2.9	3
125	Liquid state dependent solidification of a Co-B eutectic alloy under a high magnetic field. Journal of Materials Science and Technology, 2022, 116, 58-71.	10.7	3
126	Effect of the kinetic model on parameter distortions in non-isothermal transformations. Journal of Alloys and Compounds, 2009, 479, L22-L25.	5.5	2

#	Article	IF	CITATIONS
127	Deformation Micromechanisms of a Ti-Based Metallic Glass Composite with Excellent Mechanical Properties. Materials Science Forum, 0, 745-746, 809-814.	0.3	2
128	Revealing the Local Microstates of Fe–Mn–Al Medium Entropy Alloy: A Comprehensive First-principles Study. Acta Metallurgica Sinica (English Letters), 2021, 34, 1492-1502.	2.9	2
129	Formation of core-shell structure in immiscible CoCrCuFe1.5Ni0.5 high-entropy alloy. Materials Letters, 2022, , 132452.	2.6	2
130	Enthalpy recovery and its effect on homogeneous flow stress during supercooled liquid region for Ti40Zr25Ni8Cu9Be18 bulk metallic glass. Journal of Non-Crystalline Solids, 2011, 357, 3049-3052.	3.1	1
131	Diffusion Bonding of Fe-Based Amorphous Ribbon to Crystalline Cu. Materials Science Forum, 2013, 745-746, 788-792.	0.3	1
132	Relationship between grain boundary diffusion in nanocrystals and amorphous microstructure. Surface and Interface Analysis, 2016, 48, 1341-1344.	1.8	1
133	Soldering of Zr-based bulk metallic glass and copper by Au–12Ge eutectic alloy. Rare Metals, 2019, 38, 52-58.	7.1	1
134	Investigation of atomic diffusion at Ni/Zr 48 Cu 36 Ag 8 Al 8 interfaces in the glass transition temperature. Surface and Interface Analysis, 2021, 53, 135-139.	1.8	1
135	The Localized Corrosion and Stress Corrosion Cracking of a 6005A-T6 Extrusion Profile. Materials, 2021, 14, 4924.	2.9	1
136	The Nanocrystal and Its Thermal Stability in Ti ₄₀ Zr ₂₅ Ni ₈ Cu ₉ Be ₁₈ Metallic Glass during Homogeneous Deformation. Materials Science Forum, 2011, 688, 431-436.	0.3	0
137	EFFECT OF HEATING TYPES ON THE UNDERCOOLED SOLIDIFICATION MICROSTRUCTURE OF Co76Sn24EUTECTIC ALLOY. , 2016, , 649-656.		0
138	Oxygen-Induced Mechanical Property Variations of Rapidly Solidified Ti-Based Bulk Metallic Composites. Journal of Materials Engineering and Performance, 2019, 28, 5793-5796.	2.5	0
139	Interactions Between TiAl Melt and Crucibles Material during Casting Process. , 2013, , 2669-2678.		0